# CHAPTER 6: ORGANIC PETROLOGICAL AND GEOCHEMICAL RESULTS

# Chapter 6

# Organic Petrological and Geochemical Results

## 6.1 Organic Petrology: Coal Macerals

All the main groups of macerals (vitrinite, inertinite and liptinite) are observed within the Labuan sediments. The liptinite in these sediments are sporinite, cutinite and suberinite. Also, secondary liptinite macerals occur, such as bituminite and exsudatinite. The inertinite group of macerals are in relatively low abundant compared to other groups. The following sections describe the maceral distribution at each location.

### 6.1.1 Tg. Punei unit

The samples studied are liptinite-poor. The liptinitic macerals observed include cutinite which displays yellow fluorescence and occurs as cylindrical bodies with serrated margins. All the liptinitic macerals are dark grey in colour but show a yellowish orange to light brown colour under blue irradiation (Plate 6.1). Vitrinite mainly is detrovitrinite. The Inertinite present is mainly micrinite. Pyrite is present as framboids surrounded by micrinite (Plate 6.2).

### 6.1.2 Richardson Point unit

These show ground mass vitrinite. Bodies of resinite inside vitrinite are observed. The resinite occurs as oval and spherical shaped bodies. They are dark grey to brown under white light. Under blue light they show greenish yellow fluorescence. Inertinite is not observed in the samples studied (Plate 6.3).

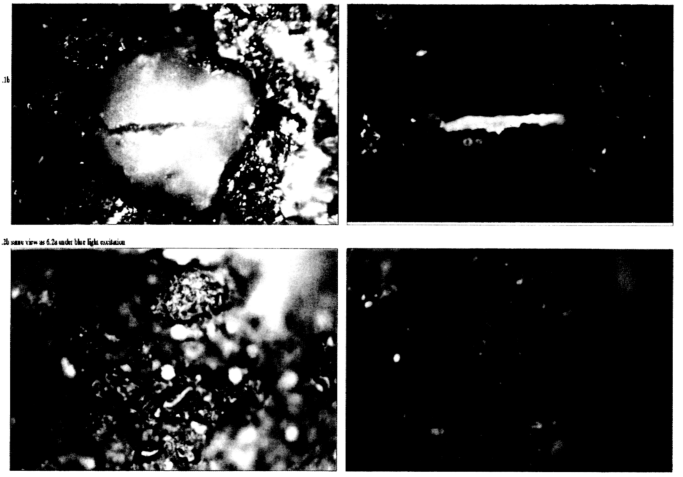

Plates 6.1: Vitrinite occurring with micrinite (M) and cutinite (C) in sample Lab 21
Plates 6.2: Vitrinite particles showing pitted (patchy) appearance with common occurrence of micrinite (M) and framboidal pyrite (P) in sample Lab 21

The low abundance of liptinite in both Tg. Punei and Richardson Point units may be explained by the expulsion of oil from liptinite macerals at a relatively lower maturity level or the original particles lacking in the liptinite macerals.

### 6.1.3 Temiang unit

The sample study from the Setap Shale from this location shows abundant vitrinite. Inertinite is not observed in this sample. Liptinite macerals are presented and are mainly bituminite, cutinite and exusdatinite, which exudates from bituminite exsudatinite (see Plates 7.1)

### 6.1.4 East Kiamsam Sandstone

The sample studied from this unit shows an abundance of vitrinite and an absence of inertinite. The liptinite macerals present in this sample are bituminite and suberinite (Plates 6.4). The shape of suberinite is irregular which may be due to the early oil generation from this maceral.

### 6.1.5 Tg. Batu unit

Only minor vitrinite is observed within Belait Formation at Tg. Batu. In this unit, there is bitumen wisps present in the samples studied.

### 6.1.6 Layang Layangan unit I

The samples of Layang Layangan unit I, south of Tg. Layang Layangan and OKK Daud, contains vitrinite, liptinite and inertinite.

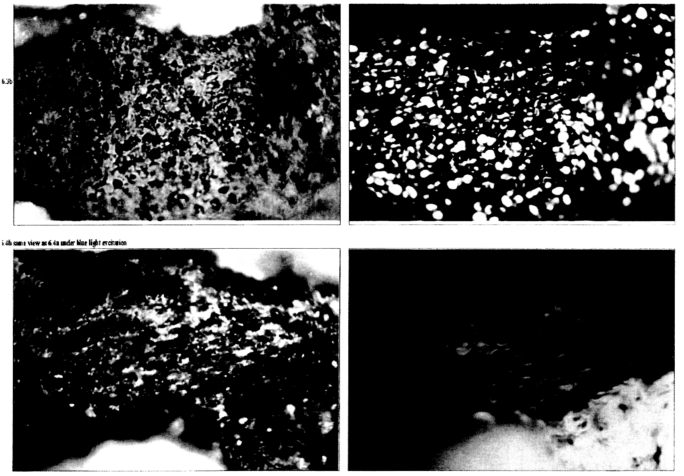

Plates 6.3: Resinite occurs as oval-to-round bodies filling cell lumens in sample Lab 18.
Plates 6.4: Framboidal pyrite associated with practically disordered subernite of sample Lab 23.

The vitrinite is unstructured and occurs as tellinite, or collinite. These units are relatively rich in liptinitic macerals such as cutinite (Plates 6.5) and sporinite (plates 6.8). Sporinite occurs as disc-shaped or elongated thread-like bodies. Resinite occur in this unit as large bodies compared to other macerals.

Resinite is found rounded and elongated bodies having yellowish fluorescence (Plates 6.6). According to Teichmuller (1989) this maceral is not only derived from resins but also from a range of other chemicals such as balsams, latexes, fats, and waxes. Secondary liptinitic macerals, such as bituminite and exsudatinite, have also been observed in this unit. Bituminite occurs in amorphous forms (Plates 6.7). Bituminite has been described by Teichmuller (1974) as an amorphous liptinite maceral having no definite shape and size. In this study it occurs and as finely dispersed lenses, streaks and, at time, as a ground mass for other liptinite macerals.

All of the liptinite macerals observed are brown to dark under reflected white light and show yellow to yellow brownish fluorescence under blue light. The inertinite macerals are relatively low in content compared to vitrinite or liptinite. The macerals of this group are dominated by sclerotinite (Plates 6.5). Bitumen wisps occur within the shaley beds (Plates 6.8and 6.9).

Pyrite occurs in several forms such as veins and framboids (Plate 6.5)

### 6.1.7 Layang Layangan unit II

Layang layangan unit II at Tg. Layang Layangan and Tg. Kubong are relatively vitrinite rich. The vitrinite appears to be brittle and is at times affected by cracks and fractures possibly induced during coalification processes (Plate 6.10) or may by tectonics (Plate 6.11). These fractures are filled with exsudatinite, which may develop into a network upon hydrocarbon expulsion. The fracturing seems to have a preference

for particular areas of the vitrinite probably due to the nature of the vitrinite which may, in turn, depend on the original plant species and components.

The liptinite present are suberinite, exsudatinite, resinite and fluorinite (Plate 6.13 & 6.14). Inertinite macerals are rare in this unit and are mainly sclerotinite (Plate 6.14). Pyrites occur as framboids associated with oil expulsion (Plate 6.11 & 6.13).

### 6.1.8 Bethune Head unit

In the Bethune Head unit, the pyrite is only observed in vitrinite and occurs in elongated form. The bitumen staining occurs within the shaley material.

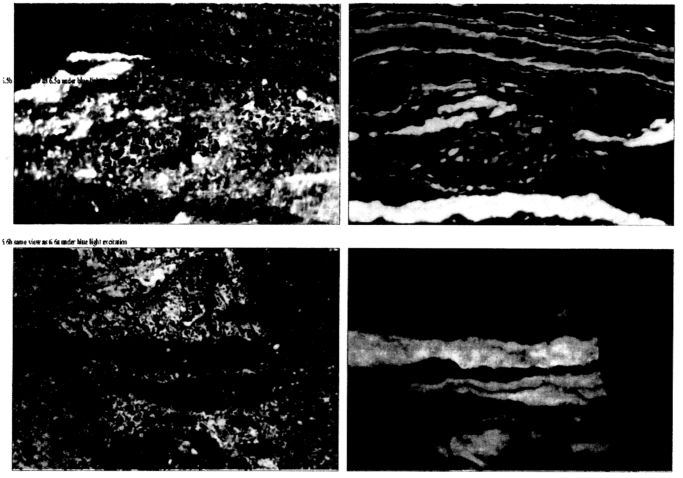

Plates 6.5: Cutinite (C), (Sb) exsudatinite (E) filling sclerotinite (Sc), fluorinite (F) voids and pyrite veins (P) in sample Lab 7
Plates 6.6: Resinite (R) within vitrinite (V) in sample Lab 37

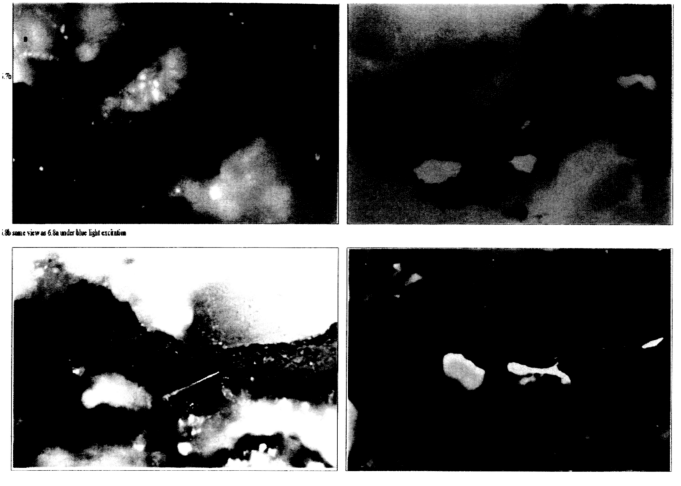

Plates 6.7: Vitrinite particles (V) and bituminite. The bituminite is characterise by lacking of definite shape or structure and may shows high fluorescence when impregnated with oil staing. The plates also show bitumen staing within shaley materials fluorescing intense yellow. (sample Lab 5).
Plates 6.8: Vitrinite particles (V) and sporinite (Sp) rimmed by yellowish brown fluorescing bitumen sating. (sample Lab 4).

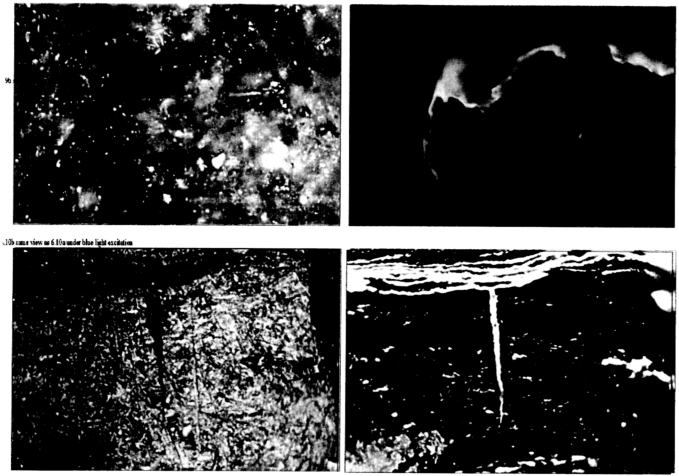

Plates 6.9: Bitumen wisps staing within shaley materials (sample Lab 36).
Plates 6.10: Exsudatinite (E) exudates from suberinite (Sb) and fill crack. The plates show other liptinitic macerals (e. g. liptodetrinite within vitrinite groundmass (sample Lab 7).

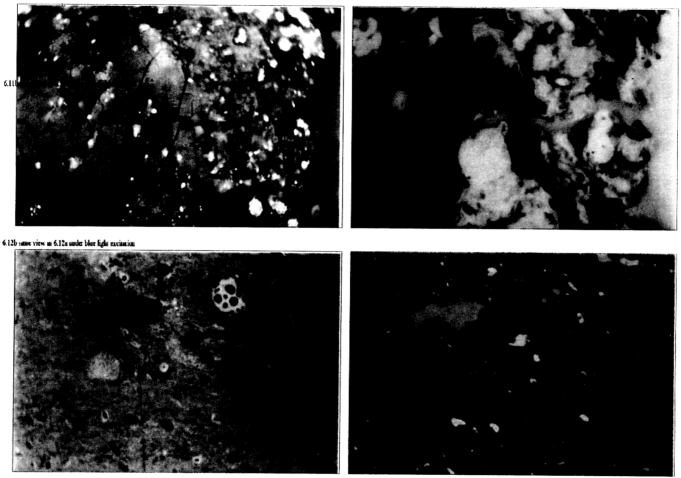

Plates 6.11: Fractured vitrinite partly filling by expelled oil (bitumen) (O). These plates show presence of framboidal pyrite (P). In sample Lab 2

Plates 6.12: Bituminite (B) display brownish yellow fluorescence and characterise by of lack any shape or structure, while sporinite (Sp) shows bright yellow fluorescence. Other liptinitic macerals present are liptodetrinite and exsudatinite (E) that occur as cell filling with scleritonite (Sample Lab 10)

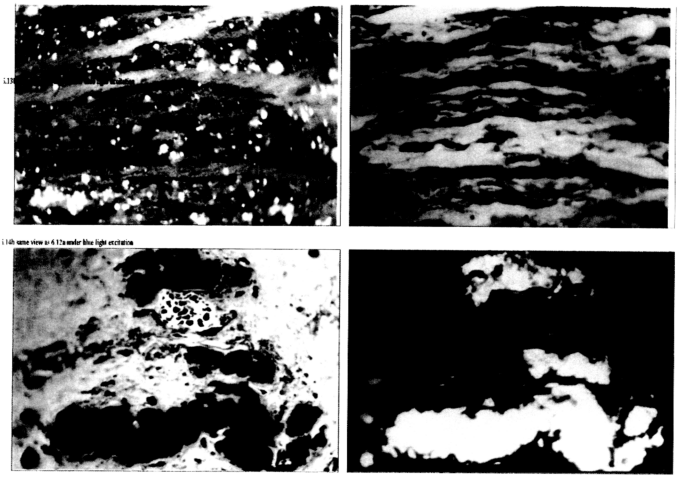

Plates 6.13: Common occurrence of framboidal pyrite (P) associated with fluorinite (F) in sample Lab 2
Plates 6.14: Resinite (B) within Vitrinite (V) and Exsudatinite filling sclerotinite(S) in sample Lab 10

**6.2 Vitrinite Reflectance**

Despite a number of problems (e.g. Hunt. 1995), vitrinite reflectance remains the most widely used indicator of thermal stress. Its applicability extends over a longer maturity range than any other indicator, and experienced petrologists can make a large number of analyses in relatively short time.

In coal samples, the reflectance measurements are made only on the telocollinite of the vitrinite group of coal macerals. For shale this is not always possible, therefore readings are made on other vitrinitic particles. All the measurements carried out in this study are shown in Table 6.1 (see also Figure 6.1). Histograms for these data are in appendix

The vitrinite reflectance measurements show higher readings for Tg. Punei samples of than the others. The vitrinite data of Tg. Punei unit range from 0.68 to 0.80%Ro.

The data for the Richardson Point unit is 0.56%Ro, for this massive shale and siltstone from the Temiang unit is 0.55%.Ro, while the vitrinite reflectance for Tg. Batu unit is about 0.60%Ro.

The samples studied from Layang Layangan unit I show vitrinite reflectance ranging from 0.52%Ro to 0.49%.Ro. The lower vitrinite reflectance values measured on these units are related to the position of samples within the stratigraphic sequence. It should be noted that this unit was grouped within Temburong Formation by Mazlan (1994).

The vitrinite reflectance for a single sample of Layang Layangan unit II at Tg. Layang Layangan is 0.49%Ro, while the sample from Tg Kubong is 0.48%Ro. These

units, which make up the prominent strike ridge from Tg. Layang Layangan to Tg. Kubong, are considered as the base of the Temburong formation by Mazlan (1994), and Base of Upper Belait by Lee (1977); Wilson (1964).

The vitrinite reflectance of the shallow marine sample which occupies the upper part of Belait Formation (Wilson, 1964; Lee, 1977; Mazlan, 1994/97, Tongkul, 2001) at Bethune Head is 0.46% Ro

| Sample No. | Description | Formation (Lee, 1977) | No. Reaging | R min (%) | R max (%) | R mean (%) | Stand.-Dev. |
|---|---|---|---|---|---|---|---|
| **Lab 26a** | Shale | Belait Formation | 20 | 0.56 | 0.62 | 0.60 | 0.015 |
| **Lab 17** | Shale | | 30 | 0.40 | 0.47 | 0.44 | 0.019 |
| **Lab 10** | Coal | | 52 | 0.45 | 0.51 | 0.48 | 0.016 |
| **Lab 2** | Coaly Sandstone | | 20 | 0.42 | 0.55 | 0.49 | 0.036 |
| **Lab 37** | Siltstone | | 31 | 0.45 | 0.57 | 0.49 | 0.030 |
| **Lab 5** | Siltstone | | 30 | 0.41 | 0.59 | 0.50 | 0.058 |
| **Lab 32** | Siltstone | | 32 | 0.43 | 0.59 | 0.52 | 0.049 |
| **Lab 39** | siltstone | | 25 | 0.51 | 0.60 | 0.56 | 0.030 |
| **Lab 23** | Siltstone | East Kiamsam Sandstone | 25 | 0.51 | 0.64 | 0.58 | 0.048 |
| **Lab 18** | Siltstone | Temburong Formation | 25 | 0.51 | 0.62 | 0.56 | 0.034 |
| **Lab 21** | Coal | | 25 | 0.65 | 0.69 | 0.68 | 0.010 |
| **Lab 22** | Calcareous Coal | | 30 | 0.77 | 0.81 | 0.80 | 0.007 |

Table 6.1: Vitrinite reflectance data

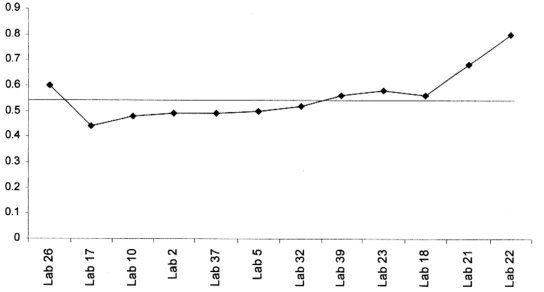


Figure 6.1: Plot of vitrinite data

### 6.3 Organic Geochemistry: Biomarker Data

Molecular parameters used in the current study, including isoprenoids, normal-alkanes, and triterpanes, are presented in Table 6.2 with peak identification shown in Table 6.3. The analyses of samples studied show variations in term of biomarker parameters (Figure 6.2). However, Biomarkers distributions for each location are discussed below:

#### 6.3.1 Tg. Punei unit

The Tg. Punei displays a higher abundance of low molecular weight n-alkanes compared to high molecular weight ones (Figure 6.3). The Pr/Ph ratios are high and range from 2.20 to 2.75. The ratios of higher plant derived n-alkane to algae-derived n-alkanes ($nC_{31}/nC_{17}$) ranges from 0.42 to 0.86. CPI (Carbon Preference Index) values are 1.09 in both samples studied from this formation. The $Pr/nC_{17}$ and $Ph/nC_{18}$ ratios are 0.31-0.68 and 0.11 to 0.31, respectively.

In relation to tritepanes (Figure 6.4), Tm is higher than Ts with Ts/ (Ts+Tm) ratios ranging from 0.41 to 0.32. The oleanane index is high in both samples (1.31-1.33). The $\beta\alpha/\alpha\beta$-$C_{30}$ hopane ratios are low (0.11-0.13), whilst the hopane isomeration at C-22: 22S/ (22S+22R) for $C_{31}$ and $C_{32}$ are high (0.62-0.63 and 0.57-0.59, respectively).

#### 6.3.2 Richardson Point unit

In contrast to the Tg, Punei unit, the TIC (total ion current) study of the Richardson point unit show a bimodal n-alkane (Figure 6.5). A pronounced odd preference in the $C_{23}$ to $C_{33}$ yields CPI values from 1.20 to 1.32. Pristane/Phytane ratios are relatively high in all samples, ranging from 3.31 to 4.57.

| Sample number | Lithology | Unit | $nC_{15}/nC_{17}$ | CPI | Pr/Ph | $Pr/nC_{17}$ | $Ph/nC_{18}$ | $\frac{Tx}{(Tx+Tm)}$ | $Ole/C_{30}H$ | $C_{29}N/C_{30}H$ | $Mor./C_{30}H$ | $C_{31}\frac{S}{(S+R)}$ | $C_{32}\frac{S}{(S+R)}$ |
|---|---|---|---|---|---|---|---|---|---|---|---|---|---|
| Lab 26 | Shale | Tg. Batu | 0.53 | 1.25 | 2.72 | 1.48 | 0.54 | 0.39 | 0.58 | 0.65 | 0.23 | 0.58 | 0.59 |
| Lab 25 | Sandstone | | 0.71 | 1.37 | 1.59 | 0.72 | 0.37 | | 0.54 | 0.80 | 0.20 | 0.60 | 0.62 |
| Lab 17 | Shale | Bethune Head | 1.80 | 1.20 | 1.65 | 0.95 | 0.52 | 0.41 | 1.36 | 0.65 | 0.20 | 0.55 | 0.55 |
| Lab 12 | Siltstone | Layang Layangan unit II | 1.19 | 1.43 | 5.67 | 2.43 | 0.43 | 0.47 | 0.95 | 1.98 | 0.43 | 0.21 | 0.38 |
| Lab 10 | Coal | | | 1.42 | 7.50 | | | 0.05 | 0.12 | 0.47 | 0.58 | 0.35 | 0.25 |
| Lab 1 | Coaly Sandstone | | 2.13 | 2.33 | 1.63 | | | 0.17 | 0.94 | 1.74 | 0.60 | 0.34 | 0.27 |
| Lab 37 | Coaly Sandstone | | | 1.54 | 7.27 | | | 0.35 | 0.96 | 3.59 | 0.96 | 0.23 | 0.18 |
| Lab 36 | Shale | | 3.32 | 1.62 | 3.29 | 2.95 | 0.89 | 0.28 | 0.80 | 2.16 | 0.60 | 0.35 | 0.42 |
| Lab 33 | Siltstone | Layang Layangan unit I | 2.42 | 1.43 | 2.38 | 2.21 | 0.65 | 0.32 | 0.85 | 1.90 | 0.40 | 0.39 | 0.40 |
| Lab 4 | Shale | | 3.29 | 1.81 | 4.00 | 3.09 | 0.57 | | 0.81 | 1.75 | 0.42 | 0.42 | 0.39 |
| Lab 7 | Coal | | | 1.60 | 4.29 | | | 0.47 | 0.53 | 1.21 | 0.43 | 0.28 | 0.26 |
| Lab 39 | Siltstone | Temiang | 0.26 | 1.11 | 2.70 | 1.11 | 0.41 | 0.38 | 1.02 | 0.72 | 0.20 | 0.59 | 0.60 |
| Lab 41 | Shale | | 3.58 | 1.06 | 2.69 | 2.00 | 0.74 | 0.40 | 0.42 | 1.25 | 0.30 | 0.48 | 0.61 |
| Lab 23 | Siltstone | East Kiamsam Sandstone | 0.35 | 1.22 | 2.97 | 1.26 | 0.43 | 0.31 | 0.89 | 0.83 | 0.33 | 0.55 | 0.57 |
| Lab 21 | Coal | Tg. Punei | 0.42 | 1.09 | 2.75 | 0.31 | 0.11 | 0.32 | 1.31 | 0.58 | 0.13 | 0.62 | 0.59 |
| Lab 22 | Calcareous Coal | | 0.86 | 1.09 | 2.20 | 0.68 | 0.31 | 0.41 | 1.33 | 0.59 | 0.11 | 0.63 | 0.57 |
| Lab 20 | Shale | | 1.67 | 1.20 | 3.31 | 2.38 | 0.72 | 0.50 | 0.52 | 0.47 | 0.16 | 0.59 | 0.60 |
| Lab 18 | Siltstone | Richardson Point | 2.26 | 1.31 | 4.57 | 2.44 | 0.53 | 0.14 | 1.29 | 0.93 | 0.32 | 0.59 | 0.66 |
| Lab 19 | Siltstone | | 1.65 | 1.32 | 4.18 | 3.44 | 0.82 | 0.23 | 1.20 | 1.19 | 0.28 | 0.60 | 0.60 |

*CPI = {[($C_{25}$-$C_{35}$-odd No.)/($C_{24}$-$C_{34}$-even No.)] + [($C_{25}$-$C_{35}$-odd No.)/($C_{26}$-$C_{36}$-even No.)]}/2 Bray and Evans (1961);* Pr = Pristane; Ph = Phytane

Table 6.2: Normal-alkanes, isoprenoids and triterpanes parameters

| Peak | Compound | Abbreviation |
|---|---|---|
| 1 | 18α(H),21β(H)-Trismorneohopane (C27) | Ts |
| 2 | 17α(H),21β(H)-Trismorhopane (C27) | Tm |
| 3 | 17α(H),21β(H)-Norhopane (C29) | N |
| 4 | 18α(H)-Oleanane (C30) | Ole |
| 5 | 17α(H),21β(H)-Hopane (C30) | H |
| 6 | Moretane (C30) | Mor. |
| 7 | 22S-17α(H),21β(H)-Homohopane (C31) | |
| 8 | 22R-17α(H),21β(H)-Homohopane (C31) | |
| 9 | 22S-17α(H),21β(H)-Bishomohopane (C32) | |
| 10 | 22R-17α(H),21β(H)-Bishomohopane (C32) | |
| U | Unknown | |

Table 6.3: Identification of triterpanes in the m/z 191 mass fragmentograms

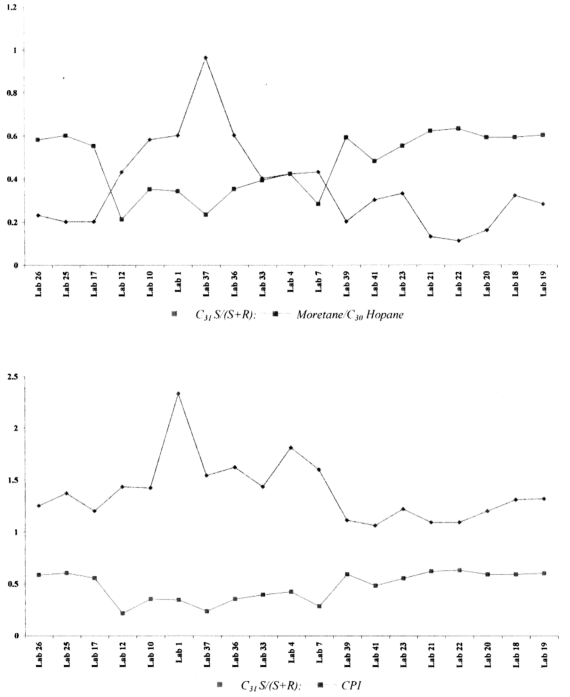


Figure 6.2: Charts show some differences between the samples studied.

The ratio of higher plant derived n-alkane (n-$C_{31}$) to algae-derived n-alkanes (n-$C_{17}$) range from 1.65 to 2.26.

The pristane to normal-alkane (n-$C_{17}$) ratios are greater than 2 (2.38 to 3.44), while the phytane to normal-alkane n-$C_{18}$) are less than 1 (0.53 to 0.82).

Figure 6.6 shows the distribution of triterpanes (m/z 191) in this unit. The hopane isomeration at C-22: 22S/ (22S+22R) for $C_{31}$ and $C_{32}$ are high and range from 0.59 to 0.60 for $C_{31}$ and for $C_{32}$ range from 0.60 to 0.66. The oleanane index is generally high: more than 1 in samples Lab 18 and Lab 19 and 0.52 for sample Lab 20. In these samples, Tm is higher than Ts as reflected in Ts (Ts + Tm) which range from 0.14 to 0.50. The ratios of moretane to $C_{30}$ hopane are low (0.16 – 0.32). The $C_{29}$ norhopane / $C_{30}$ hopane ratios range from 0.47 to 1.19.

### 6.3.3 East Kiamsam Sandstone

Only one sample was studied from this unit because of very limited exposure. The East Kiamsam Sandstone TIC distribution (sample Lab 23) is shown in Figure 6.3. From this figure, the differences between Tg. Punei unit and the East Kiamsam Sandstone. Wilson (1964) regarded these units as Temburong Formation, but Lee (1977) separated them) are clearly shown, as demonstrate in the pristane/$C_{17}$ ratio. At East Kiamsam Sandstone unit the pristane / n-$C_{17}$ ratio is 1.26 while phytane / n-$C_{18}$ is 0.43. The relative abundance of pristane is high compared to phytane, reflected in a pristane / phytane ratio of 2.97. The CPI value is high (1.22) compared to the CPI values observed in the Tg. Punei unit

In the triterpane distributions (Figure 6.4), $C_{30}$ hopane is dominant, and $C_{29}$ norhopane is high compared to the samples from the Tg. Punei unit. The oleanane / $C_{30}$ hopane is high (0.89) but less than in the Tg. Punei unit, where the oleanane dominated.

$C_{29}$ norhopane to $C_{30}$ hopane is 0.83. The Ts (Ts + Tm) ratio is low (0.31). In relation to homohopanes, the ratios 22S / (22R + 22S) for these sample are 0.55 and 0.57 for $C_{31}$ and $C_{32}$, respectively. The moretane / $C_{30}$ hopane ratio is low but is not as low as in the Tg. Punei unit.

### 6.3.4 Temiang unit

The single sample from this exposure displays a distribution similar to the East Kiamsam sandstone, typified low to medium molecular weight n-alkane with dominant peaks at $nC_{16}$ and n $C_{18}$ (Figure 6.7). The n-$C_{31}$/n-$C_{17}$ ratio is 0.26 and pristane / n-$C_{17}$ is 1.11 while phytane/n-$C_{18}$ is 0.41. The pristane/phytane ratio is high (2.70) and CPI value is low (1.11).

The triterpane distribution is dominated by oleanane in this sample (Figure 6.8). The oleanane / $C_{30}$ hopane is 1.02. $C_{29}$ norhopane / $C_{30}$ hopane is 0.72. The Ts (Ts + Tm) ratio is low (0.38).

The 22S/ (22R + 22S) at C-22 for $C_{31}$ and $C_{32}$ hopane ratios for Lab 39 are high (0.59 and 0.60, respectively), while moretane / $C_{30}$ hopane is low (0.20).

### 6.3.5 Tg Batu unit

The samples collected from outcrop at Tg. Batu, which is considered as Belait Formation in previous work (e.g. Wilson (1964); Lee (1977); Tangkul (2001)) display distributions totally different from other Belait Formation samples. They show high abundance of low molecular weight n-alkanes compared to high ones (Figure 6.7). The dominant peaks in these samples are Pr, n-$C_{14}$ and n-$C_{16}$. The pristane / Phytane ratios are 1.59 – 2.72. Pristane / n-$C_{17}$ are 0.72 – 1.48 while phytane / n-$C_{18}$ are 0.37 – 0.54.

The ratios of terrestrial derived n-alkane to marine-derived n-alkanes (n-$C_{31}$/n-$C_{17}$) are 0.53 – 0.71. The CPI value is 1.59 – 2.72.

In the distribution of triterpanes (Figure 6.8), $C_{30}$ hopane is dominant. The oleanane / $C_{30}$ hopane ratios are 0.54 – 0.58. The Ts (Ts + Tm) ratio is low (0.39). In relation to homohopane, the 22S / (22R + 22S) ratios are 0.58 – 0.60 and 0.59 – 0.60 for $C_{31}$ and $C_{32}$, respectively. The moretane / $C_{30}$ hopane ratios are 0.20 – 0.23.

### 6.3.6 Layang Layangan unit I

In contrast to the East Kiamsam Sandstone, the normal alkane distribution of the Layang Layangan unit I is dominated by the n-alkanes in the range n-$C_{13}$ to n-$C_{35-37}$ (Figures 6.9 & 6.11). The maxima of the n-alkane distribution are at $C_{31}$ and $C_{14}$. The Carbon Preference Index (CPI) values range from 1.43 to 1.81, showing a strong odd/even number predominance. Pr/ Ph ratios range from 2.38 to 7.27 in this unit. The $nC_{31}/nC_{17}$ ratios are greater than 1.0 in all samples. $Pr/nC_{17}$ ratios range from 2.21 to 3.09.

In relation to triterpanes (Figures 6.10 &6.12), the ratios 22S / (22*R* + 22*S)* of Layang Layangan unit I for $C_{31}$ hopane ranges from 0.23 to 0.42 and from 0.18 to 0.42 for the $C_{32}$ homologue. The ratios of moretane/$C_{30}$ hopanes are high and range from 0.42 to 0.96 for this unit. The high abundance of Tm compared to Ts is reflected in Ts/ (Ts+Tm) ratios, which range from 0.28 to 0.47. The oleanane index ranges from 0.53 to 0.96.

### 6.3.7 Layang Layangan unit II

The normal alkane distributions for the Layang layangan unit II are shown in Figure 6.9 (Lab 1). The TIC (total ion current) trace shows low abundance of n-alkanes

and may show slight biodegradation based on the presence of humps indicative of an unresolved complex mixture. The CPI values are more than 1, ranging from 1.42 to 2.33. The Pr/Ph ratio ranges from 1.63 to 7.50. The Pr/$nC_{17}$ ratio is about 2.43. The 22S/ (22R + 22S) at C-22 for $C_{31}$ and $C_{32}$ hopane ratios range from 0.21 to 0.35 for $C_{31}$ and from 0.25 to 0.38 for $C_{32}$. The Ts/ (Ts+Tm) ratios are 0.17 to 0.47 and oleanane index range from 0.12 to 0.95.

### 6.3.8 Bethune Head unit

The single sample from this unit displays a distribution similar to the Layang Layangan units, typified a low to high molecular weight n-alkane with dominant peaks at $nC_{31}$ (Figure 7.5). A carbon preference index (CPI) is 1.20, reflecting the predominance of odd-numbered n-alkane. The n-$C_{31}$/n-$C_{17}$ ratio is 1.80 and pristane / n-$C_{17}$ is 0.95 while phytane/n-$C_{18}$ is 0.52. The pristane/phytane ratio is about 1.65.

The triterpane distribution is dominated by oleanane in this sample (Figure 7.5). The oleanane / $C_{30}$ hopane is 1.1.36. $C_{29}$ norhopane / $C_{30}$ hopane is 0.65. The Ts (Ts + Tm) ratio is low (0.41).

The 22S/ (22R + 22S) at C-22 for $C_{31}$ and $C_{32}$ hopane ratios is high (0.55) while moretane / $C_{30}$ hopane is low (0.20).

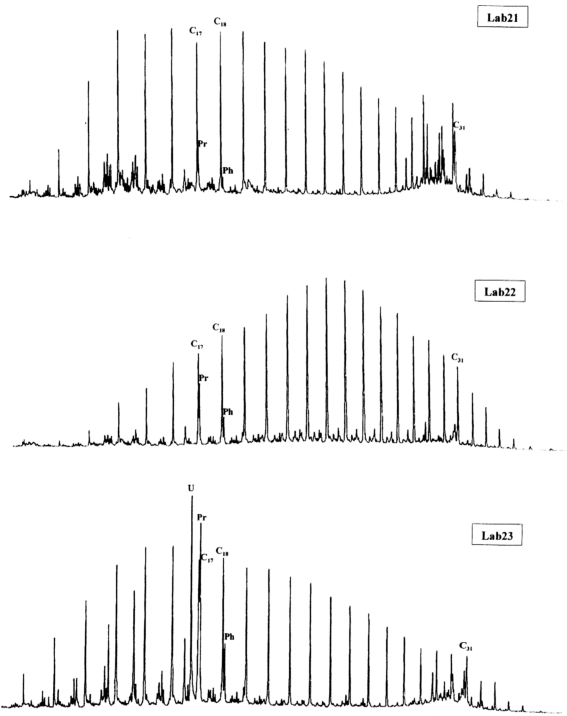


Figure 6.3: Normal-alkanes and isoprenoids distributions in Tg. Punei unit (Lab 21 & Lab 22) near to Shell Crude Oil Terminal and East Kiamsam Sandstone (Lab 23) at Tg. Kiamsam)

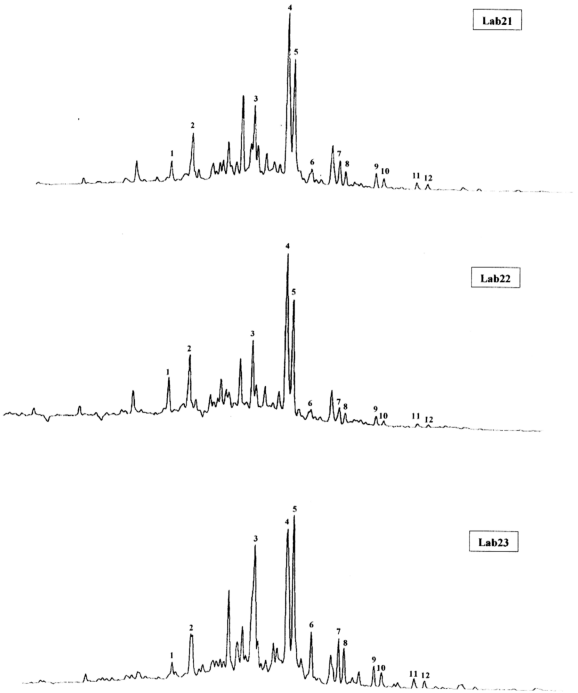


Figure 6.4: Distributions of triterpanes (m/z 191) in Tg. Punei unit near to Shell Crude Oil Terminal (Lab 21 & Lab 22) and East Kiamsam Sandstone at Tg. Kiamsam (Lab 23)

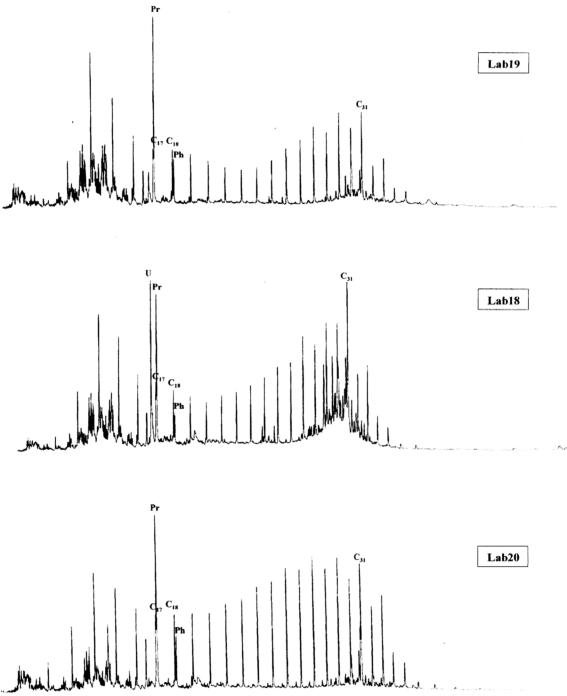


Figure 6.5: Normal-alkanes and isoprenoids distributions in Richardson Point unit

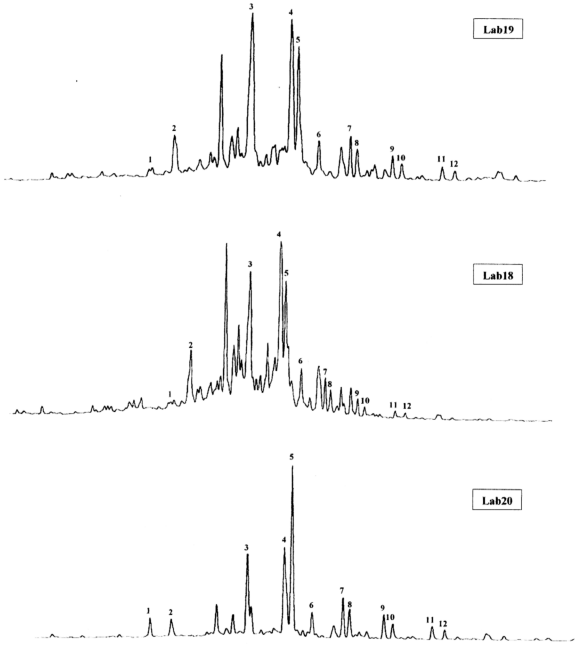


Figure 6.6: Distributions of triterpanes (m/z 191) in Richardson Point unit

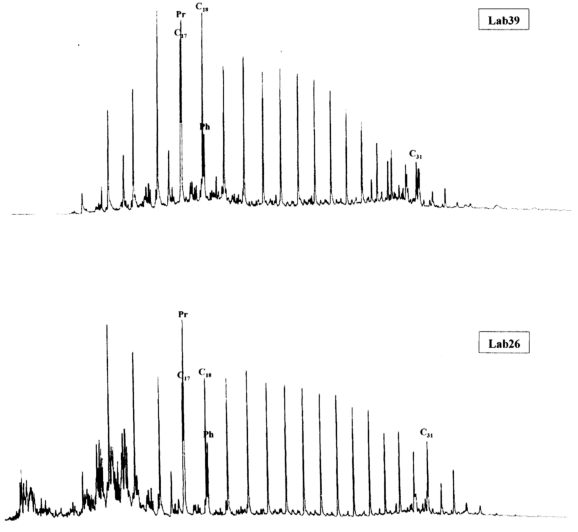


Figure 6.7: Normal-alkanes and isoprenoids distributions in Tg. Batu unit (Lab 26) and Temiang unit (Lab 39) on JLN Lubok Tmiang.

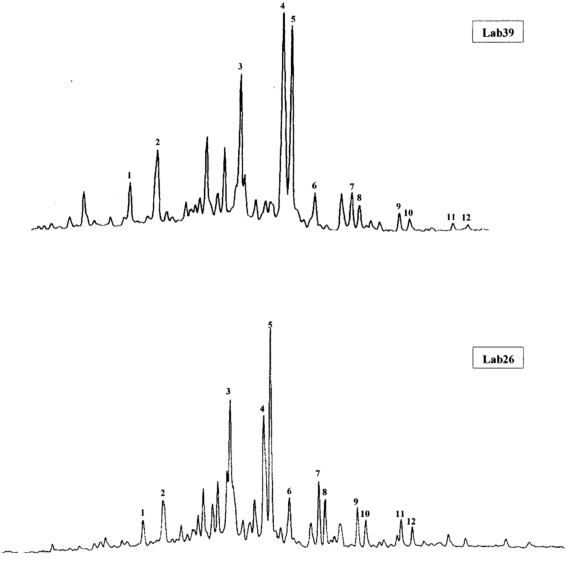


Figure 6.8: Distributions of triterpanes (m/z 191) in Tg. Batu unit (Lab 26) Temiang unit (Lab 39) at JLN Lubok Temiang.

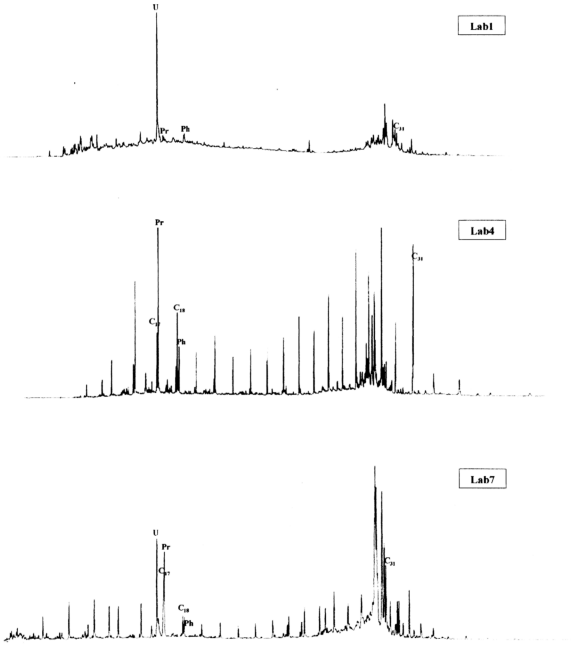


Figure 6.9: Normal-alkanes and isoprenoids distributions in Layang Layangan unit I (Lab 4 &Lab 7) and unit II (Lab 1)

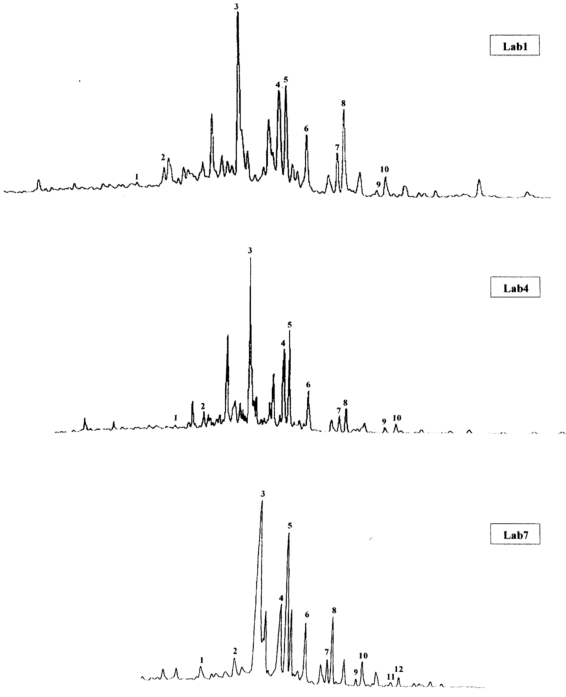


Figure 6.10: Distributions of triterpanes (m/z 191) in Layang Layangan unit I (Lab 4 & Lab 7) and unit II (Lab 1)

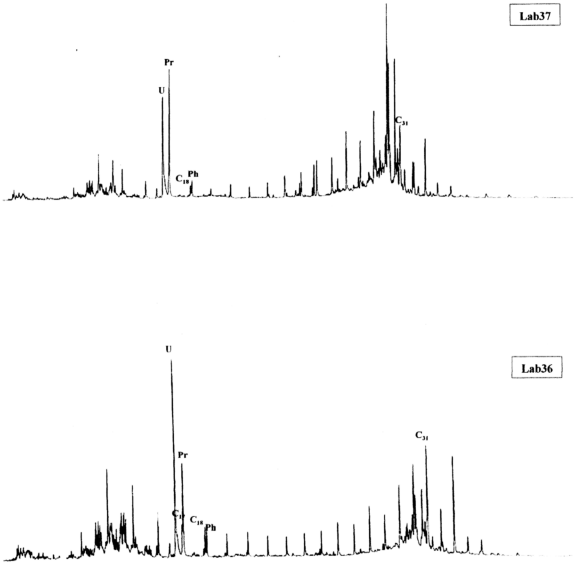


Figure 6.11: Normal-alkanes and isoprenoids distributions in Layang Layangan unit I at JLN OKK Daud.

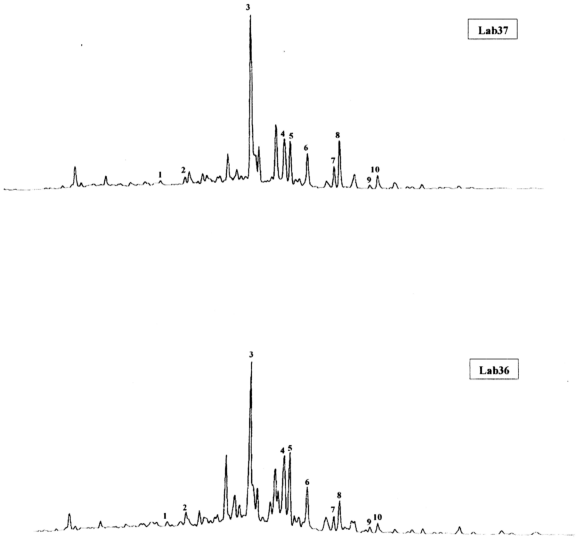


Figure 6.12: Distributions of triterpanes (m/z 191) in Layang Layangan unit I JLN OKK Daud.